ELSEVIER

Composites: Part A 33 (2002) 841–854

composites
Part A: applied science and manufacturing

www.elsevier.com/locate/compositesa

Model-assisted feedback control for liquid composite molding

Joy P. Dunkers[a], Kathleen M. Flynn[a], Richard S. Parnas[a], Dionyssios D. Sourlas[b,*]

[a]National Institute of Standards and Technology, Polymers Division, Quince Orchard and Clopper Rds., Gaithersburg, MD 20899, USA
[b]Department of Chemical Engineering, University of Missouri-Rolla, 143 Schrenk Hall, Rolla, MO 65409-1230, USA

Received 1 June 1999; revised 22 January 2002; accepted 4 February 2002

Abstract

A model-assisted feedback control algorithm, a type of generic model control, is implemented to control cure in resin transfer molding. This control algorithm calculates an apparent temperature of reaction based on the cure data input form a sensor, and this temperature is used to compare the actual rate of reaction to the desired rate and to calculate the mold set-point temperature. The model input into the control algorithm is an empirical cure model of a pre-ceramic polymer with an Arrhenius temperature dependence from 55 to 95 °C. In this work, the effect of varying control parameters is evaluated through cure simulations and experiments. Also, the effect of noise on the controller robustness is evaluated through simulation and experiment. Control parameters are evaluated for 55 and 95 °C. © 2002 Published by Elsevier Science Ltd.

Keywords: A. Thermosetting resin; A. Ceramic-matrix composites (CMCs); E. Cure; Liquid composite molding

1. Introduction

The necessity for process control during composite manufacturing has been widely recognized [1]. During the liquid molding process, injection pressure and temperature are commonly controlled to ensure part uniformity. However, the most critical parameter to assess and control would be the cure state of the polymer because it effects resin dominated end-use properties such as compression and flexure strength [2,3]. The cure is defined as the amount of reactive species present at any time during the reaction compared to the amount at time zero. Variation of the cure of a composite from the desired cure state is a result of numerous factors including improper resin/catalyst mix, resin, catalyst, and equipment aging, batch-to-batch variation of resin system and even humidity. One approach to control part quality is an integrated cure sensing and process control system. The process control system must be able to use the sensor information to make decisions about manipulation of the cure. The most common variable used to control the cure of the resin is temperature.

There are volumes of information about sensors designed to monitor resin cure directly or indirectly. Most of the sensors investigated are based upon dielectrics [4,5], ultrasonics [6], or spectroscopy [7–10]. There are advantages and disadvantages associated with each type of sensor. The choice of sensor is dictated by the properties of interest and its potential for interfacing with a control system. For example, dielectrics and ultrasonics are capable of monitoring changes in resin properties over large volumes. However, both dielectrics and ultrasonics are indirect measures of cure that require correlation with another parameter that can be related to composite quality. In dielectric measurements, conductance is roughly correlated with viscosity. However, the conductance early in cure is dominated by the presence of ions and can overwhelm the important information relating to viscosity. This phenomenon can hinder control efforts early in the cure where control is most effective and easiest to implement.

Spectroscopic sensors are commonly fiber optic and measure local resin properties [11]. In most cases, they are noninvasive and can monitor cure at the center of the part where large temperature exotherms are most common. To monitor resin cure fiber optic sensors have been developed that measure various material properties such as near-infrared attenuated total reflectance [12], near-infrared external reflection [13], refractive index [14], fluorescence [15], etc. Some fiber optic sensors even measure resin cure close to fiber surface through evanescent wave spectroscopy [16]. In this work, a mid-infrared internal reflection surface sensor based on evanescent wave spectroscopy was selected to follow the cure during the liquid molding of a thin part. The curing reaction can be followed directly using this type

* Corresponding author. Tel.: +1-573-341-6331; fax: +1-573-341-4377.
E-mail address: dsourlas@umr.edu (D.D. Sourlas).

1359-835X/02/$ - see front matter © 2002 Published by Elsevier Science Ltd.
PII: S1359-835X(02)00027-1

of spectroscopy which is effective throughout the entire cure. Knowledge of the progress of the reaction throughout the entire cure of the composite is mandatory if process control is to be implemented.

Briefly, in previous work [17], a prism surface sensor based on attenuated total internal mid-infrared spectroscopy was developed and used to remotely collect the infrared spectra of a pre-ceramic polymer injected into the resin transfer mold. Currently, the infrared beam exits the Fourier transform infrared (FT-IR) spectrometer, and a system of optics and hollow waveguides directs the beam through the ZnSe surface sensor and then to the detector. The resulting infrared spectrum is analyzed, and a number representing the cure state of the resin is computed for use in the process control computer. The process control computer runs the model-assisted feedback control algorithm and makes a control decision by inverting a kinetics model of the resin cure.

The liquid composite curing process studied in this work is a typical batch process during which the controller is required to manipulate the independent variable (temperature) so that the controlled or dependent variable (degree of cure) follows a pre-specified (set-point) trajectory. Such a trajectory is typically obtained off-line using a model system. Feedback control structures have been employed in the context of batch process control in order to achieve disturbance rejection and set-point tracking. A variety of control system design techniques have been proposed in the context of batch process control. Nonlinear cascade structures consisting of proportional and proportional/integral controllers with varying gain have been experimentally tested [18] for the control of batch reactors. Nonlinear controllers based on global input/output linearization have been developed and compared to conventional proportional/integral/derivative types for typical polymerization reactors [19]. More recently, input/output linearization has been employed in order to synthesize nonlinear cascade structures [20]. Through simulation and experiments, the aforementioned studies have demonstrated improved control performance compared to conventional linear designs. Other approaches to the control of batch processes are based on on-line optimization techniques coupled with state estimation [21]. Research investigations have also focused on various process control aspects of resin cure in composites manufacturing such as on-line optimization-based control of the cure cycle of composite laminate materials [22], model predictive control with parameter estimation and model adaptation in liquid composite molding [23] and control of the injection pultrusion process using flow, heat transfer and cure process models [24].

In the present paper, real-time sensing of the chemistry of the process is integrated with feedback control in order to achieve set-point tracking and disturbance rejection throughout the curing process. The primary output is the remaining monomer (degree of cure), which is measured using infrared spectroscopy. The ability to obtain real-time chemistry measurements eliminates the need for nonlinear state estimation in this problem. The secondary measurement is the temperature of the curing chamber. The two measurements are utilized in a cascade structure whereby the deviation of the measured degree of cure from its set-point determines the desirable temperature set-point. The control algorithm employed in this primary loop is conceptually similar to generic model control approaches [25]. A simplified cure model based on isothermal cure experiments is employed to relate system temperature to the expected remaining monomer. The temperature set-point is then obtained via a control algorithm that requires solution of nonlinear equations. This work considers the behavior of this primary control loop through simulation and experiment. The effect that noise in the cure measurements has on the performance of the controller is also examined.

2. Experimental

2.1. Materials

The Blackglas™ 493A resin system was used as-received from Allied-Signal (Des Plains, IL). The catalyst systems were used in this study. The 493B catalyst system was mixed as 2 pph by weight in the 493A monomer. A platinum cyclovinyl complex, mass fraction of 2–3% Pt in cyclic vinylmethylsiloxanes, was used as a second catalyst as-received from Hüls America (Piscataway, NJ). This commercial catalyst was mixed as 0.4 pph in 493A. For all curing experiments, the 493A resin and catalyst system were mixed at room temperature before heating.

2.2. Instrumentation

FT-IR spectra were taken using a Nicolet Magna 550 FT-IR spectrometer equipped with mercury–cadmium–telluride (MCT-A) detector and a nitrogen purge. A heatable ZnSe horizontal attenuated total internal reflection (HATR) accessory was used for the process control experiments as a convenient surface sensor and mold since the sensor was previously demonstrated in a composite molding experiment [17]. Experiments performed with the HATR accessory were done with 8 cm^{-1} resolution and 32 co-added scans with a 5 min delay between spectra at 55 °C and 2 min delay between spectra at 95 °C. The room temperature resin was injected into the pre-heated HATR accessory for the kinetic experiments.

The acquisition of spectra was automated using a macro programmed from the Omnic 1.2a software. Using this macro, the spectra are collected and saved. The areas of the peaks of interest are computed and stored into a file. This macro calls two Quickbasic executable files. The first executable program sends the time to the process control computer through a serial-to-serial port connection. The second executable program reads the peak areas from the

file. The computer calculates remaining monomer and sends this index to the process control computer. The reactive and internal standard peaks used to monitor the reaction are the Si–H stretching peak (2155 cm^{-1}) and a methyl group deformation peak (1245 cm^{-1}). In this study, the total collect and data processing time before the index is sent to the process control computer in approximately 1.5 min. The collection and processing time is small compared to the total cure time of 5 h.

The control algorithm was programmed in Quickbasic and executed on a laptop i486 computer for this prototype mold and sensor system. After each spectrum, the temperature set-point was manually adjusted on the temperature controller to the output temperature from the process control algorithm. Manual adjustment of the set-point temperature is acceptable since the cure is slow. The simulated control experiments were programmed in Visual Basic.

3. Results and discussion

3.1. Process description

The processing equipment includes a mold, a pump used to inject the resin into the mold as well as sensors and actuators for the base-level temperature control loop. The fluid pressure at the mold inlet and outlet are regulated permitting programmed injection profiles. Pressure control is achieved by connecting the fluid injection and the fluid overflow pressure pots to both high- and low-level pressure source through three-way solenoid valves. Vacuum pressure transducers mounted at the mold inlet and the mold outlet obtain pressure measurements required by the pressure controllers. The pressure controllers are resident in the process control computer but are run on a stand-alone data acquisition and co-processor board. This internalized arrangement of the pressure controllers was chosen to permit very close co-ordination between the base-level pressure control and a planned high-level controller for flow control in multi-port molds.

The mold is heated electrically, and a stand-alone controller regulates the amount of electrical power supplied to the mold. Temperature measurements are supplied to the controller by resistance temperature devices mounted in the mold wall and within the part itself. Any one of the temperature signals may be chosen to be the measured variable for the controller. All the measured temperatures are relayed to the main control computer for further manipulation, if required. Large temperature gradients may require additional manipulations to choose an appropriate set-point temperature to download to the stand-alone controller. The set-point for the temperature controller is set remotely from the control computer, and the set-point is determined by the cure controller resident in the computer.

3.2. Process and controller model development

Cure data is usually given in terms of amount of material reacted (degree of cure) or the amount of remaining material (remaining monomer). In our work, experiments were conducted with a polysiloxane resin, and kinetic model of that resin was developed for use in the control algorithm and the simulations. The kinetic model used by the controller consists of a function F that was fit by a double exponential model of the form

$$A(t) = F(C, t, T) = A_0(c_1\, e^{-k_1 t} + c_2\, e^{-k_2 t}) \quad (1)$$

where $A(t)$ is the monomer concentration at time t, A_0 is the initial monomer concentration, c_1 and c_2 are weighting factor, and k_1 and k_2 are reaction rate constants [28]. Additionally, the reaction rate constants were fit to Arrhenius expressions to include the temperature dependence of the reactions

$$k_i = k_{i,o} \cdot e^{-\Delta H_i/(RT)}, i = 1, 2 \quad (2)$$

where ΔH_i is the activation energy, $k_{i,0}$ is the frequency factor of the reaction rate constant, and the subscript i can be either 1 or 2. The vector, C, of kinetic constants shown in Eq. (1) is defined as $C = (c_1, c_2, k_{1,0}, k_{2,0}, \Delta H_1, \Delta H_2)$. The double exponential form of the kinetic model is sufficiently complex to demonstrate the ability of the controller to invert many types of kinetic models, and such changes in rate behavior are common in polymerizing systems at high conversion due to the onset of diffusional limitations [29].

Desirable process operation is defined in terms of a desirable reference cure trajectory (programmed cure, $A_p(t)$) that the system should follow. This reference trajectory corresponds to the temporal evolution of a model system under constant temperature (programmed temperature, T_p) and is described by Eq. (1) for a given parameter vector C. Disturbances lead to variations in the parameters in C, i.e. the actual system has parameter values other than the nominal model system used to obtain the reference trajectory. Hence, when the (constant) programmed temperature T_p is applied to the actual system, the resulting temporal evolution of the cure will be different than the desirable one (i.e. the programmed cure $A_p(t)$). The problem is addressed in this work through the design of a cascade feedback control system. The control problem is defined as follows. Manipulate the mold temperature so that the actual remaining monomer follows a given reference cure trajectory in the presence of disturbances. The remaining monomer is the primary measurement and is employed by the primary controller in order to determine the set-point for the secondary loop that regulates the system temperature. The design of the primary controller is the focus of the section. Standard linear control techniques can be employed to design the secondary controller.

Let $A_a(t)$ be the measured (apparent) remaining monomer at time t. $A_a(t)$ will in general be different from the programmed remaining monomer, $A_p(t)$, which corresponds to the reference trajectory. The isothermal kinetic model, Eq. (1), is inverted by the control algorithm to obtain the

apparent temperature $T_a(t)$:

$$A_a(t) = F(C, t, T_a(t)) \Rightarrow T_a(t) = F^{-1}(C, t, A_a(t)) \quad (3)$$

where the exponent (-1) indicates inversion (i.e. solution) of the nonlinear equation.

In practice, the inversion indicated in Eq. (3) is performed via a numerical procedure which computes the solution, $T_a(t)$, within some pre-specified tolerance. The apparent temperature, $T_a(t)$, corresponds to the constant polymerization temperature necessary for the system to match the apparent and programmed remaining monomer amounts at time t. The apparent temperature is a fictitious quantity that depends on time. If $A_a(t) = A_p(t)$, then the apparent and programmed temperatures at time t are equal. Assume that over the entire range of remaining monomer values, the temperature affects the degree of cure in a monotonic manner. This is true for $c_1\Delta H_1$, $c_2\Delta H_2$ positive since a straightforward calculation demonstrates that based on Eq. (1), and under such conditions, $dF/dT < 0$ for all times. The above conditions hold for our model. Hence, increasing the processing temperature results in reduced amounts of remaining monomer for the same processing time. Then, the temperature set-point can be selected so that the tracking objectives are met. During a chemical reaction, increasing the processing temperature decreases the amount of remaining monomer. Thus if, $A_a(t) < A_p(t)$ (achieved reaction more than the programmed), $T_a(t) > T_p$ is implied. Provided that the real process follows Eq. (1) for different, but unknown, parameter values (C), one can safely postulate that a reduction in the processing temperature will slow down the reaction so that in the future, the difference $A_a(t) - A_p(t)$ decreases. If $A_a(t) > A_p(t)$, the processing temperature should increase to improve tracking of the reference trajectory. The following generic expression is suggested to update the processing temperature set-point value

$$T_{sp}(t + \Delta t) - T_{sp}(t) = H_1(T_p - T_a(t)) \quad (4)$$

where H_1 is a potentially nonlinear bounded function such that

$$H_1 : R \to R, x \in R \to H_1(x)\begin{cases} > 0 & \text{if } x > 0 \\ = 0 & \text{if } x = 0 \\ < 0 & \text{if } x < 0 \end{cases} \quad (5)$$

where R is the set of real numbers.

In summary, Eq. (4) combined with Eq. (3) defines a feedback control algorithm which uses composition measurements, $A_a(t)$, to compute the desirable temperature set-point for the interval, $t + \Delta t$. This control algorithm does not consider differences in the reaction rate between the reference model (programmed trajectory) and the process. Incorporation of such information in the control algorithm, Eq. (4), will generally improve control quality. This task is tackled next.

The process model in Eq. (1) can be differentiated with respect to time, and an expression for the incremental change in the degree of curve over a time interval Δt can be obtained:

$$G_1(C, t, T_p) \triangleq \frac{\partial F}{\partial t} \approx \frac{A_p(t) - A_p(t - \Delta t)}{\Delta t}. \quad (6a)$$

Alternatively, Eq. (1) can be written at time t and $t - \Delta t$ and ratioed to provide an equivalent expression for the change in the degree of curve over the time interval Δt:

$$G_2(C, t, T_p) \triangleq \frac{A_p(t)}{A_p(t - \Delta t)} = \frac{F(C, t, T_p)}{F(C, t - \Delta t, T_p)} = e^{-k_1 \Delta t} \frac{1 + \frac{c_1}{c_2} e^{t(k_1 - k_2)}}{1 + \frac{c_1}{c_2} e^{(t - \Delta t)(k_1 - k_2)}}. \quad (6b)$$

Employing the apparent cure values in Eqs. (6a) and (6b), a new quantity called instantaneous temperature $T_i(t)$ can be defined

$$\frac{A_a(t) - A_a(t - \Delta t)}{\Delta t} = G_1(C, t, T_i(t)) \Rightarrow T_i(t) = G_1^{-1}\left(C, t, \frac{A_a(t) - A_a(t - \Delta t)}{\Delta t}\right) \quad (7a)$$

or

$$\frac{A_a(t)}{A_a(t - \Delta t)} = G_2(C, t, T_i(t)) \Rightarrow T_i(t) = G_2^{-1}\left(C, t, \frac{A_a(t)}{A_a(t - \Delta t)}\right) \quad (7b)$$

$T_i(t)$ is analogous to $T_a(t)$. Eqs. (7a) and (7b) need not result in the same instantaneous temperature value. In this work, Eq. (7b) is used within the control algorithm. If the real process parameter vector C is identical to the one employed in Eqs. (1), (6a) and (6b), the $T_i(t)$ is equal to T_p and is constant. In general, the instantaneous temperature will be a function of time, and the difference $T_i(t) - T_p$ is a measure of the difference between the process and the model trends. As a result, with this measure the generic control law (Eq. (4)) is extended as follows

$$T_{sp}(t + \Delta t) - T_{sp}(t) = H_1(T_p - T_a(t)) + H_2(T_p - T_i(t)) \quad (8)$$

where H_2 is potentially a nonlinear bounded real valued function that is similar to H_1, since the monotonicity properties G_2 with respect to T are similar to the corresponding properties of F.

A simplified version of Eq. (8) that is used in this work employs a linear right-hand side

$$T_{sp}(t + \Delta t) - T_{sp}(t) = \omega_1((T_p - T_a(t)) + \omega_2(T_p - T_i(t))) \quad (9)$$

where T_{sp} is the temperature set-point downloaded to the base-level temperature controller, and ω_1 and ω_2 are tuning constants. When both the degree of cure, $A_a(t)$, and the rate

of change of A_a equal the programmed quantities at the same time, the apparent temperatures, T_a and T_i, will equal the programmed temperature, T_p and Eq. (9) indicates that no change in the system temperature is required. There are more elaborate ways of using the apparent kinetic temperatures including model-based predictive control with or without model adaptation [23], but the model-assisted feedback control algorithm described earlier is expected to be adequate for the slow-curing chemical system under current consideration.

In practice, physical constraints limit both the allowable and achievable temperature values for the system. Furthermore, since Eq. (9) has characteristics of an integrator, appropriate measures should be taken in order to avoid the possibility of reset windup. As a result, and in the spirit of 'conditional integration', the following alternative to Eq. (9) is actually implemented

$$T_{new} = T_{sp}(t) + \omega_1[(T_p - T_a(t)) + \omega_2(T_p - T_i(t))],$$

$$T_{sp}(t + \Delta t) = \begin{cases} T_u & \text{if } T_{new} \geq T_u \\ T_{new} & \text{if } T_l < T_{new} < T_u \\ T_l & \text{if } T_{new} \leq T_l \end{cases} \tag{10}$$

where T_u and T_l are pre-defined, fixed, upper and lower temperature set-point bounds. These bounds can be selected based on material limitations.

The studies undertaken in this work focus on the effect of the two tuning parameters in Eqs. (9) and (10) on the achieved tracking. In Sections 3.3–3.5 that follow some more information is provided regarding the well-posedness of the proposed control algorithm as well as implementation issues.

3.3. Control system analysis

The cascade feedback configuration consists of an inner temperature loop, which is considered, in this discussion to be stable. In order to implement the 'master' control algorithm (Eqs. (9) and (10)), the existence of the inverses in Eqs. (3) and (7b) should be demonstrated. This is possible with the help of the inverse function theorem [27], which establishes that inversion of F (and G_2) is possible provided that the function is continuously differentiable with respect to temperature, T, and this derivative is nonvanishing.

3.3.1. Calculation of the apparent temperature $T_a(t)$ via Eq. (3)

The derivative of F with respect to its third argument, T, can be computed as follows:

$$\frac{\partial F(C,t,T)}{\partial T} = \frac{-1}{T^2}\left(c_1 k_1 t \frac{\Delta H_1}{R} e^{-k_1 t} + c_2 k_2 t \frac{\Delta H_2}{R} e^{-k_2 t}\right). \tag{11}$$

Hence, $\partial F(C,t,T)/\partial T$ is negative (and nonzero) for all times provided that $(c_i \Delta H_i) > 0$, $i = 1, 2$, which holds.

The inversion of F in Eq. (3) is not feasible for any value, $A_a(t)$, of the measured monomer concentration. At time $t > 0$, Eq. (3) has a solution provided that the following inequality holds

$$F_l(C,t) \triangleq \lim_{T\to\infty} F(C,t,T) < A_a(t) < A_0 \tag{12}$$

where the quantity $F_l(C,t)$ is computed for the reference model given by Eq. (1), and it is equal to:

$$F_l(C,t) = A_0(c_1 e^{-k_{1,0}t} + c_2 e^{-k_{2,0}t}).$$

Provided that Eq. (12) holds, then it follows that Eq. (3) will give a finite value for the apparent temperature, which is also unique.

In cases where the measurement contains a lot of noise, or when there is significant parameter deviation between the process and the reference model (given by Eq. (1)), it is possible that the bounds in Eq. (12) could be violated. If the upper bound is violated, which can only be possible due to the presence of noise, then the calculation of $T_a(t)$ is not performed and the previous set-point value is maintained (Section 3.4). To cope with violations of the lower bound, we define $F_{l,\varepsilon}(C,t) = F_l(C,t) + \varepsilon < A_0$, for some positive ε. The calculation of the apparent temperature $T_a(t)$ is now modified as follows:

$$T_a(t) = \begin{cases} F^{-1}(C,t,A_a(t)) & \text{if } A_0 > A_a(t) > F_{l,\varepsilon}(C,t) \\ F^{-1}(C,t,F_{l,\varepsilon}(C,t)) & \text{if } A_a(t) \leq F_{l,\varepsilon}(C,t) \end{cases}. \tag{13}$$

Eq. (13) practically imposes a maximum value on the apparent temperature. This bound is equal to the apparent temperature that corresponds to $F_{l,\varepsilon}(C,t)$. Since $F_{l,\varepsilon}(C,t) > F_l(C,t)$, this upper bound is always finite. Thus, the computed apparent temperature values will satisfy $0 < T_a(t) \leq F^{-1}(C,t,F_{l,\varepsilon}(C,t) < \infty)$ for all t.

3.3.2. Calculation of the instantaneous temperature $T_i(t)$ via Eq. (7b)

First the derivative of G_2 with respect to T is calculated to determine the sign of this derivative for different times. For $t \ggg \Delta t$ ($t - \Delta t \approx t$, $2t - \Delta t \approx 2t$), the expression for the derivative is simplified as follows:

$$\frac{\partial}{\partial T}(G_2(C,t,T)) = \frac{\partial}{\partial T}\left(\frac{A_a(t)}{A_a(t-\Delta t)}\right)$$

$$\approx \frac{-\Delta t A_0^2}{T^2 F^2(C,t-\Delta t,T)}\left\{e^{-k_1 2t} c_1^2 k_1 \frac{\Delta H_1}{R} + e^{-k_2 2t} c_2^2 k_2 \frac{\Delta H_2}{R} + e^{-k_1 t - k_2 t} \frac{c_1 c_2}{R}(k_1 \Delta H_1 + k_2 \Delta H_2)\right\}.$$

As a result, G_2 is a decreasing function of the temperature or, equivalently, the derivative of G_2 with respect to T is negative and nonzero. Then, there exists a unique solution

of Eq. (7b) (i.e. instantaneous temperature) provided that the following inequality is satisfied:

$$G_{2,1}(C,t) < \frac{A_a(t)}{A_a(t-\Delta t)} < 1. \tag{14}$$

The quantity on the left of Eq. (14) is defined as:

$$G_{2,1}(C,t) \triangleq \lim_{T\to\infty} G_2(C,t,T) = e^{-k_{1,0}\Delta t}\frac{1+\dfrac{c_2}{c_1}e^{t(k_{1,0}-k_{2,0})}}{1+\dfrac{c_2}{c_1}e^{(t-\Delta t)(k_{1,0}-k_{2,0})}}.$$

When Eq. (14) is violated, there exist no solutions of Eq. (7b). To guard against this possibility, we proceed as in the previous case of the calculation of the apparent temperature. In particular, if the upper bound of Eq. (14) is violated, the calculation of the instantaneous temperature is not performed and the application of Eq. (10) includes only the terms that depend on $T_a - T_p$ provided that T_a can be calculated (Section 3.4). To prevent difficulties due to violations of the lower bound of Eq. (14), the quantity $G_{2,1,\varepsilon}(C,t)$ is introduced such that $G_{2,1,\varepsilon}(C,t) \triangleq G_{2,1}(C,t) + \varepsilon < 1$ and ε is a given positive number. Then, the computation of the instantaneous temperature $T_i(t)$ can be modified to improve robustness:

$$T_i(t) = \begin{cases} G_2^{-1}\left(C, t, \dfrac{A_a(t)}{A_a(t-\Delta t)}\right) & \text{if } 1 > \dfrac{A_a(t)}{A_a(t-\Delta t)} > G_{2,1,\varepsilon}(C,t) \\ G_2^{-1}(C,t,G_{2,1,\varepsilon}(C,t)) & \text{if } \dfrac{A_a(t)}{A_a(t-\Delta t)} \le G_{2,1,\varepsilon}(C,t) \end{cases} \tag{15}$$

This modified calculation of the instantaneous temperature also imposes an upper bound on the computed value of $T_i(t)$ (see Section 3.3 on $T_a(t)$).

Remark. During the simulation and experimental studies performed in this work, the lower bounds defined in Eqs. (12) and (14) were never violated. This is expected since they correspond to limiting behavior at high temperature, which is beyond what is actually observed, even in the case of significant parameter deviations. Their advantage is that these conditions allow establishing bounds on the calculated apparent (Eq. (13)) and instantaneous (Eq. (15)) temperatures, which facilitates the stability analysis that follows.

3.3.3. Stability of the closed loop

Stability is established in the L_∞ sense as this is defined by Vidyasagar [26]. This property establishes that all signals in the closed loop remain finite, and they are bounded by an a priori known quantity. Due to the chemical characteristics of the system, all concentration quantities are trivially finite and a priori bounded (resin is only consumed up to elimination). Hence, the focus is on the various temperature signals (actual and computed).

L_∞ stability of the closed loop requires that the following holds:

$$\exists \Delta (0 < \Delta < \infty) \text{ such that } \max\left\{\begin{matrix} \|T(t)\|_\infty, & \|T_{sp}(t)\|_\infty, \\ \|T_a(t)\|_\infty, & \|T_i(t)\|_\infty \end{matrix}\right\} \le \Delta. \tag{16}$$

It remains to provide an estimate for the parameter Δ.

For L_∞-stable and linear inner temperature loop (mapping T_{sp} to actual mold temperature T) it follows that there exist positive constants α and β such that

$$\|T(t)\|_\infty \le \alpha\|T_{sp}(t)\|_\infty + \beta$$

where $\|\cdot\|_\infty$ is the infinity (maximum) norm.

Based on the last expression and on Eqs. (10), (13) and (15), it follows that the bound Δ should satisfy:

$$\max\left\{\begin{matrix} (\alpha|T_u| + \beta), & (\alpha|T_l| + \beta), & |T_u|, & |T_l|, \\ \|F^{-1}(C,t,F_{l,\varepsilon}(C,t))\|_\infty, & \|G_2^{-1}(C,t,G_{2,l,\varepsilon}(C,t))\|_\infty \end{matrix}\right\} \le \Delta < \infty. \tag{17}$$

The max on the left-hand side is finite for finite time intervals because of continuity with respect to time and the kinetic properties of the system. The above estimates, and the stability properties they imply, are valid in the presence of noise.

3.4. Process simulation

Simulations were conducted to verify the efficacy of the above control algorithm in preparation for implementation on the processing hardware. The simulation accounted for the limited heating and cooling rates possible on the processing equipment but assumed an isothermal programmed cure cycle (i.e. T_p = constant) and negligible spatial temperature gradients in the mold. Thus, the thermal model of the process predicts the mold temperature at time t as $T(t)$ according to

$$T(t) = \begin{cases} T_{sp}(t) & \text{if } -r_c\Delta t < T_{sp}(t) - T(t-\Delta t) < r_h\Delta t \\ T(t-\Delta t) + r_h\Delta t & \text{if } T_{sp}(t) - T(t-\Delta t) > r_h\Delta t \\ T(t-\Delta t) - r_c\Delta t & \text{if } T(t-\Delta t) - T_{sp}(t) > r_c\Delta t \end{cases}$$

where r_h is the maximum heating rate, r_c is the maximum cooling rate, and the Δt is the simulation time step. Since the controller forces the system into a nonisothermal pathway, Eq. (1) could not be used directly to simulate the cure process. Rather, Eq. (6b) was employed to compute $A(t + \Delta t)$ given the value of $A(t)$ and $T(t)$.

The set of kinetic parameters C_s used in the simulation model may be different than the set C used in the controller model. For the purpose of simulation disturbances in the chemical kinetics, $C_s \neq C$ was specifically implemented.

A limited set of simulations were conducted to assess the behavior of the controller under perfect measurement conditions, however, the experimental measurements of A were

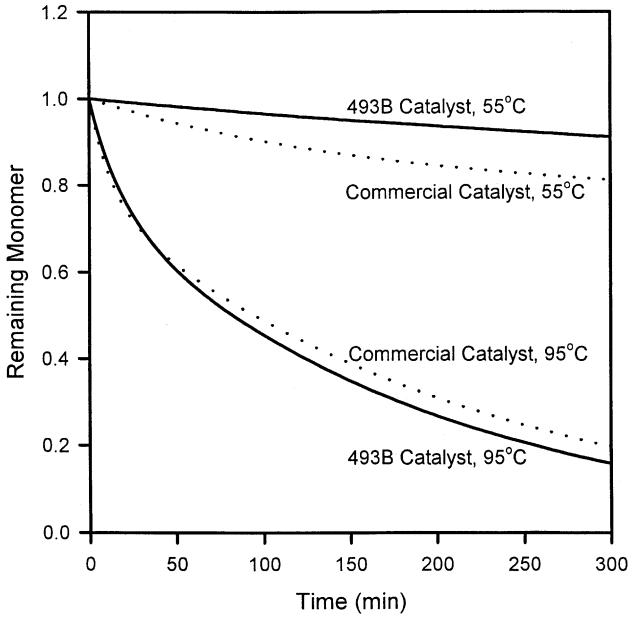

Fig. 1. Examples of isothermal cure data used to generate the kinetic equations.

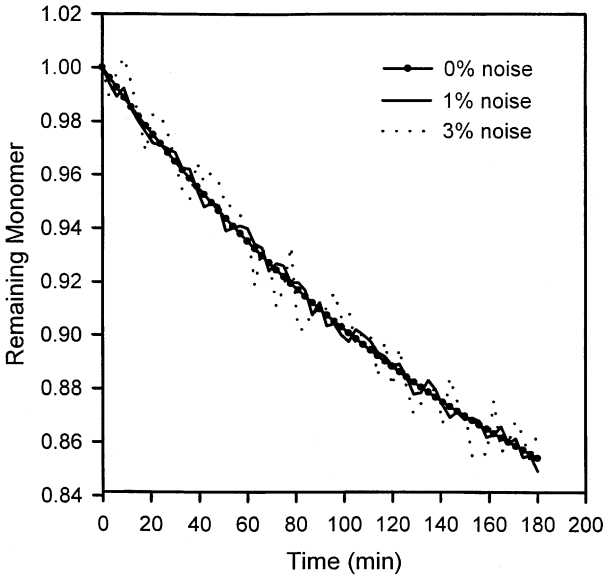

Fig. 2. A cure simulation at 55 °C with 493B catalyst and varying amounts of random noise.

found to contain small amounts of noise and uncertainty. To assess the impact of noise on the controller, small random numbers were added to the computed value of $A(t + \Delta t)$ to provide the simulated value of the measured concentration of remaining monomer in the mold

$$A_s(t + \Delta t) = A(t + \Delta t) + N_s(\Gamma(t) - 0.5)$$

where $\Gamma(t)$ is the appropriate value chosen from a string of pseudorandom numbers generated on the computer, 0.5 is subtracted from Γ to provide both positive and negative numbers, and N_s is the scaling factor used to adjust the noise level. The pseudorandom numbers were generated with the algorithm included in Visual Basic and are designed to simulate white noise. Several strings of such numbers were tested by taking discrete Fourier transforms and flat power spectral densities were obtained. Discrete autocorrelations also showed that the same strings of numbers were uncorrelated [30]. To accommodate the presence of noise, a deadband was included in the control algorithm. The deadband limits are calculated according to:

$$A_p(t) - \frac{D}{2} \leq A_s(t) \leq A_p(t) + \frac{D}{2} \tag{18}$$

If the value of the stimulated cure, A_s, satisfied Eq. (18), then no control action is executed.

The inclusion of noise may lead to instances where a part of or the entire controller was not executed, because no physically meaningful solution existed (see earlier section for quantitative justification). Since the control algorithm is based on chemical kinetics, it should be emphasized that the controller was turned off for reasons relating to the fundamental of chemical reactions and not relating to controller robustness. The first instance occurs when the measured or simulated degree of cure is greater than 1 (i.e. $A_s(t)/A_0 > 1$). In the instance, no real value of apparent temperature can be found that would reverse the progress of the reaction. Thus, when a cure signal greater than 1 is sent to the process control computer, the entire controller is not executed. A second case is encountered when the cure increases during a time step due to the presence of noise (i.e. $A_s(t + \Delta t) > A_s(t)$). In that case, Eq. (7b), which calculates the instantaneous apparent temperature, T_i, has no solution although Eq. (3) can still be solved to T_a. Thus, under those conditions, a value of T_a is computed, a value of T_i is not, and a new temperature set-point is generated with Eq. (10) based only on the difference, $T_a - T_p$.

3.5. Simulation results

Examples of cure data used to generate the kinetic equations (Eqs. (1) and (2)) for the control algorithm and simulations are shown in Fig. 1. The isothermal cure profiles shown are for 55 and 95 °C, and results for both the 493B and the commercial catalyst systems are displayed. At 55 °C, the commercial catalyst is much more effective in promoting the reaction. The cure curves at 95 °C demonstrate the complex kinetics of this system. Initially, the 493B catalyzed cure progresses more slowly than the cure catalyzed by the commercial catalyst, until about 35% conversion. Then, the rate of cure with the commercial catalyst becomes slower than for the 493B catalyst. The reaction catalyzed by the 493B material progressed further after 300 min than the reaction with the commercial catalyst. The control algorithm described earlier can effectively control the changing reaction rate at 95 °C. For most of the results in this work, the cure with the 493B catalyst will be the reaction to be controlled to the cure profile of the commercial catalyst.

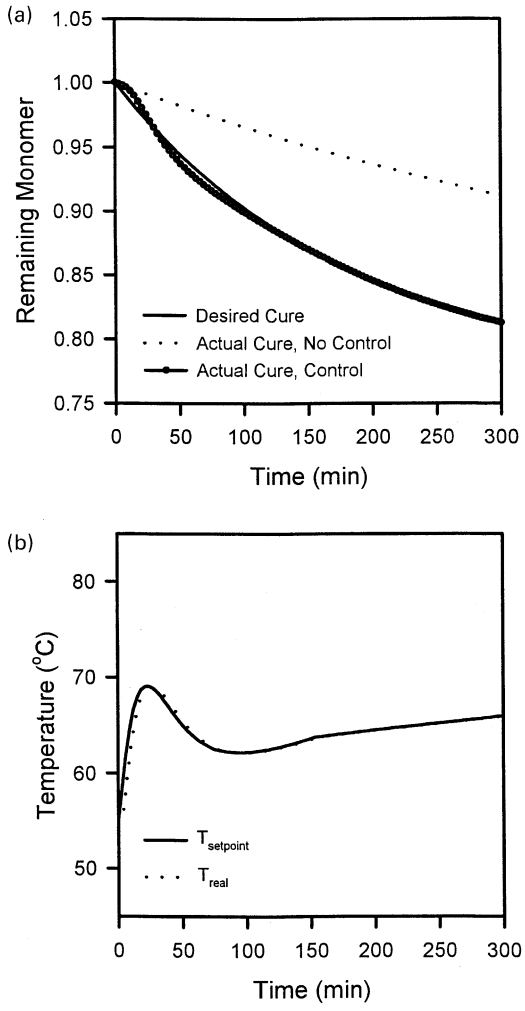

Fig. 3. A control simulations with no noise. The simulation was executed with $r_h = 5$ °C/min, $r_c = 2$ °C/min, and the tuning constants, ω_1 and ω_2, were 0.30 and 0.25, respectively. (a) Remaining monomer with and without control. (b) Temperature profile required for control.

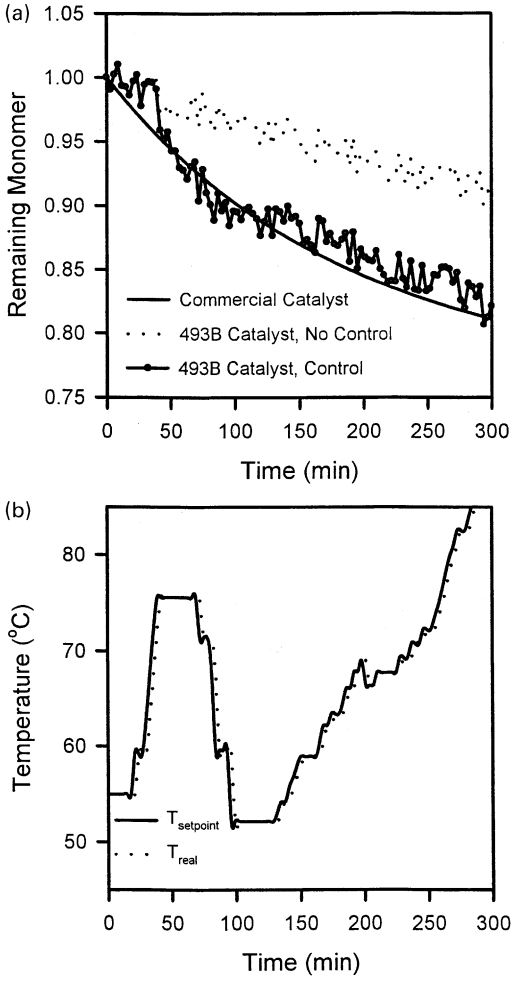

Fig. 4. A control simulation with 3% noise and deadband, executed with the same values of r_h, r_c, ω_1 and ω_2 as in Fig. 3. (a) Remaining monomer with and without control. (b) Temperature profile required for control.

The introduction of noise into a process can severely damage its controllability if it is not properly compensated for in the control algorithm. Fig. 2 shows a cure simulation at 55 °C with 493B catalyst and varying amounts of random noise. In simulations, noise was added or subtracted randomly up to one-half the amount designated for the noise level. For example, the amount of remaining monomer could vary up to ±0.5% for a 1% noise level. A noise level between 1 and 2% was determined to be the amount of noise present in HATR sensor data.

The difficulty in controlling a process with noise is shown in Figs. 3 and 4. The control simulation in Fig. 3 contains data with no noise, while the simulation in Fig. 4 contains 3% noise and deadband. All simulations were performed with an infinite heating and cooling rate. (The experimentally achievable heating (6 °C/min) and cooling (4 °C/min) rates can be classified as 'infinite' since they have the same average C_R as the infinite heating and cooling rates as verified by stimulations for a 2% noise level). The tuning constants, ω_1 and ω_2, for both simulations were 0.30 and 0.25, respectively. Both conversion curves follow the same general trend. However, the noisy cure data in Fig. 4 does not follow the desired cure pathway as closely as the data in Fig. 3. The cure pathway in Fig. 4 jumps in and out of the deadband range throughout the simulation. Also, the temperature changes called for in the simulation with 3% noise are larger and less smooth than in the 0% noise case. Such large temperature changes may be expected to cause large temperature gradients within the part, not described by the simplified simulation, which would lead to nonuniform curing and residual stresses. For the cases described here, in which the noisy signal is not filtered, this control algorithm is most effective when the deadband is set equal to the noise level. Setting a deadband smaller than the noise level leads to large controller instability and poorer control quality than for the case where those two parameters are set equal to each other. Setting the deadband larger than the noise level can smooth the required temperatures changes but only with a further degradation in control quality.

The values of the tuning parameters, ω_1 and ω_2, defined

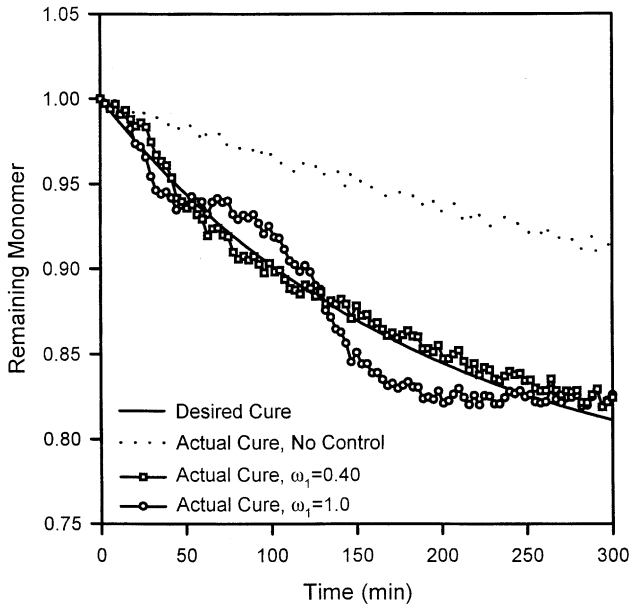

Fig. 5. Illustration of the effect on control quality by varying ω_1 while holding ω_2 at a value of 0.25, with 1% noise, at 55 °C.

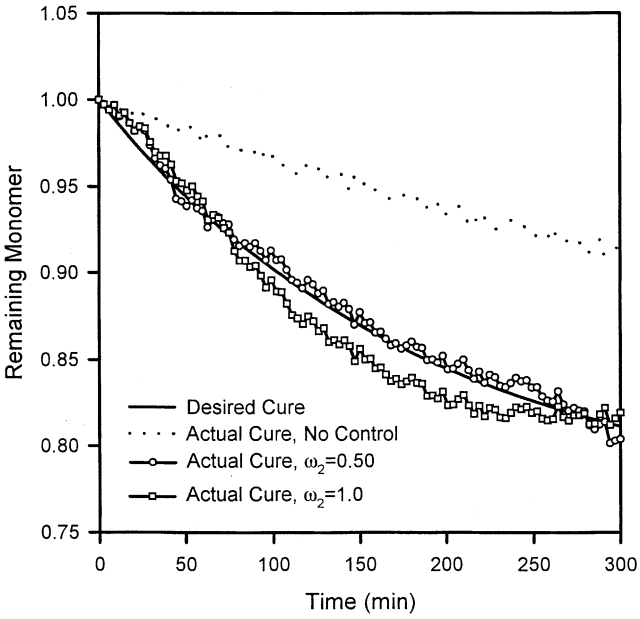

Fig. 6. Illustration of the effect on control quality by varying ω_2 while holding ω_1 at a value of 0.25, with 1% noise, at 55 °C.

in Eq. (9), should be assessed for the best controller performance. The necessity of tuning the controller arises from the imperfection of the model used in the controller algorithm. In addition to error introduced by the kinetics model, the limited heating and cooling rates are not accounted for in the control model. The best values for ω_1 and ω_2 may not be the same throughout the temperature range of interest. This problem may be resolved by setting these values to a compromise value for the entire temperature range or by varying them as a function of temperature. Fig. 5 demonstrates the effect on control quality by varying ω_1 while holding ω_2 at a value of 0.25 with 1% noise at 55 °C. The cure data with $\omega_1 = 0.4$ proceeds much closer to the desired cure profile than the data with $\omega_1 = 1$. In Fig. 6, $\omega_2 = 0.5$ is more effective in meeting the desired cure profile than $\omega_2 = 1$; while holding $\omega_1 = 0.25$, the noise level at 1%, and the temperature at 55 °C. The presence of noise affects the calculations of T_i, sometimes calling for large swings in the temperature set-point. Thus, the value of ω_2, which determines the contribution of T_i to the control output, must be adjusted to suit both the expected noise level and temperature.

The variability in controller effectiveness that was demonstrated in the previous two figures can be quantified by a dimensionless number, hereafter referred to as controller robustness (C_R)

$$C_R = \frac{\sum_{t\geq 0} (A_p(t) - A_s(t))^2_{Contr}}{\sum_{t\geq 0} (A_p(t) - A_s(t))^2_{NonContr}}$$

where $A_p(t) - A_s(t)$ is the difference between the remaining monomer for the desired cure and the actual remaining monomer at a particular time during the experiment. These differences are squared to obtain a positive number and summed over the entire experiment. The number in the numerator is a result of an experiment with control. This number is normalized by the number without control in the denominator. The simulations to determine the values for the numerator and the denominator were run with the same string of pseudorandom numbers when noise was included in the calculations. For example, a C_R number of 0.01 means that the quality of control was 100 times better than for the situation without any control. Thus, the smaller the value of C_R, the better the control quality.

The controller robustness is characterized in Fig. 7 as a function of ω_1 and ω_2 at 55 °C and 0% noise for the case where the commercial catalyst gives the desired cure behavior. As is shown in this figure, control quality is degraded at the extremes of controller parameters. From the 3D surface plot, the settings which produce a maximum is controller efficiency are $\omega_1 = 0.5$ and $\omega_2 = 0.7$. However, the control quality is still good at $\omega_1 = 0.5$ throughout the range of ω_2. The controller robustness is characterized in Fig. 8 as a function of ω_1 and ω_2 at 95 °C and 0% noise. The best control is achieved by using $\omega_1 = 0.77$, and $\omega_2 = 0.25$, but ω_1 in the range 0.6–1 provides very good control for values of ω_2 less than 0.35 and greater than 0.15. Over the entire range of control parameters, the 55 °C simulations achieve better control (lower C_R) than the 95 °C simulations.

The presence of sensor noise degrades the control quality. The controller performance is characterized as a function of noise level at 55 °C in Fig. 9 using essentially optimal control parameters ($\omega_1 = 0.50$, and $\omega_2 = 0.25$). As the noise level increases, the deadband, D, also increases so that $N_s = D$ in all cases. Five pairs of simulations were

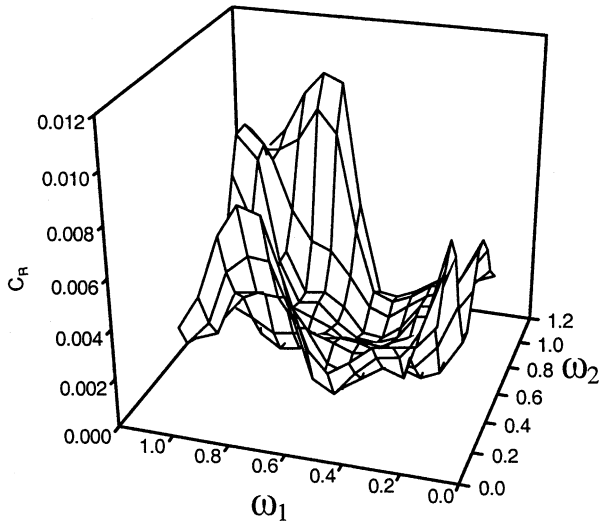

Fig. 7. The controller robustness as a function of ω_1 and ω_2 at 55 °C and 0% noise for the case where the commercial catalyst gives the desired cure behavior. Control quality is degraded at the extremes of controller parameters. The optimum settings are $\omega_1 = 0.5$ and $\omega_2 = 0.7$.

performed for each noise level to obtain values of C_R. The data points are the average values of C_R, and the error bars are the standard error from each data set. At 55 °C, the controller significantly improves the system performance even at 10% noise. Similar results to those shown in Fig. 9 are shown in Fig. 10 at a temperature of 95 °C. At 1% noise, the C_R values for 55 and 95 °C are comparable, with $C_R = 0.012$ at 55 °C and $C_R = 0.018$ at 95 °C. However, for 3% noise level, the value of $C_R = 0.11$ at 95 °C and $C_R = 0.033$ at 55 °C. The more rapid degradation in controllability at 95 °C could be at least partially compensated for by decreasing the control interval at 95 °C. Presently, both the 55 and 95 °C simulation data are run at 3 min control intervals.

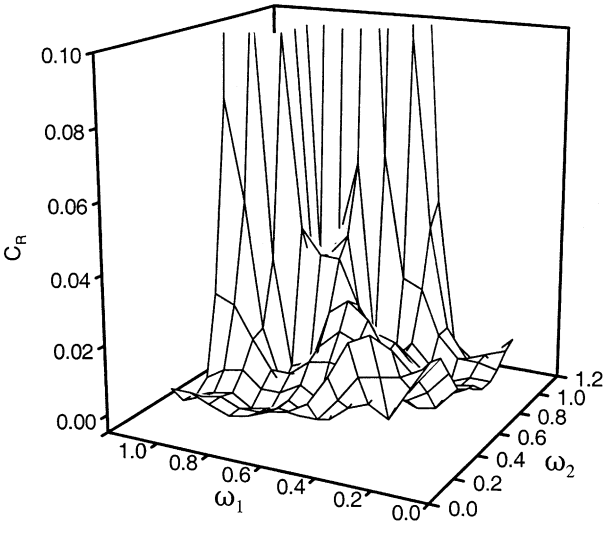

Fig. 8. The controller robustness as a function of ω_1 and ω_2 at 95 °C and 0% noise. The best control is achieved by using $\omega_1 = 0.77$ and $\omega_2 = 0.25$, but ω_1 in the range 0.6–1 provides very good control for values of ω_2 less than 0.35 and greater than 0.15.

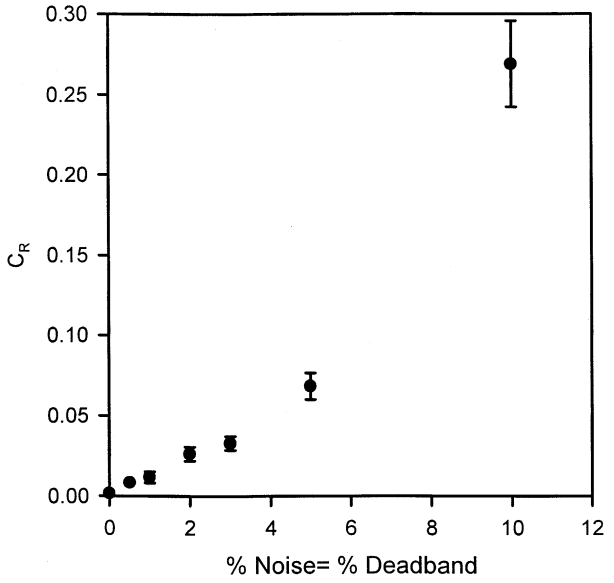

Fig. 9. The controller performance is characterized as a function of noise level at 55 °C using essentially optimal control parameters ($\omega_1 = 0.50$ and $\omega_2 = 0.25$). As the noise level was increased, the deadband, D, was also increased so that $N_s = D$ in all cases. Five pairs of simulations were performed for each noise level to obtain values of C_R. The data points are the average values of C_R, and the error bars are the standard error from each data set.

Fig. 11 is an example of the controller behavior at 55 °C where the desired cure (493B catalyst) runs slower than the actual cure (commercial catalyst). In these simulations, the initial temperature adjustments require cooling whereas the initial adjustments were heating in the simulations

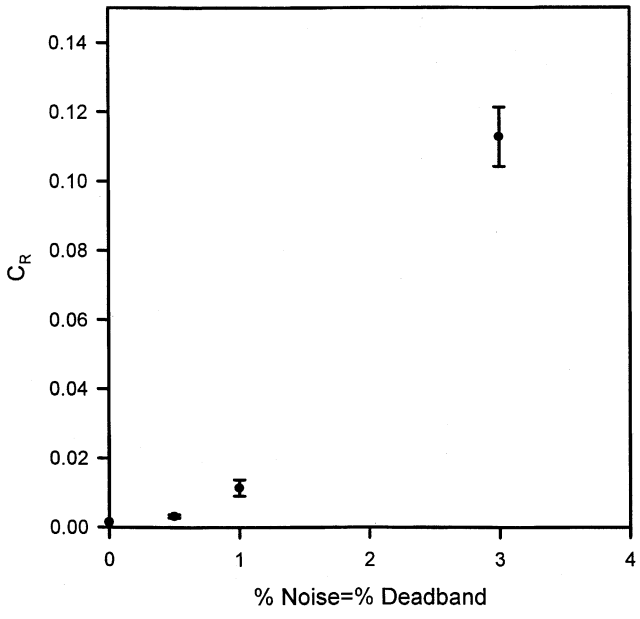

Fig. 10. The controller performance is characterized as a function of noise level at 95 °C using essentially optimal control parameters. As the noise level was increased, the deadband, D, was also increased so that $N_s = D$ in all cases.

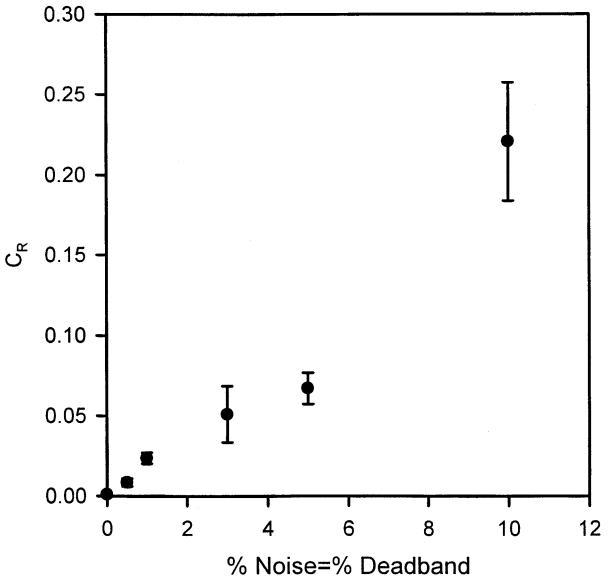

Fig. 11. An example of the control behavior at 55 °C where the desired cure (493B catalyst) runs slower than the actual cure (commercial catalyst), the opposite of the previous simulations.

described in Figs. 9 and 10. The robustness of the controller is comparable to the robustness in Fig. 9 where the commercial catalyst is designated the desired cure, even with the discrepancy in the rate of temperature set-point adjustment.

The effect of noise on the optimal values ω_1 and ω_2 is an important remaining issue. Fig. 12 displays the C_R for various values of ω_1 and ω_2 around the best values of $\omega_1 = 0.77$ and $\omega_2 = 0.25$ for 95 °C simulations. The controller robustness degrades with the addition of only 1% noise, as illustrated by the data with $\omega_1 = 0.77$ and $\omega_2 = 0.25$ when

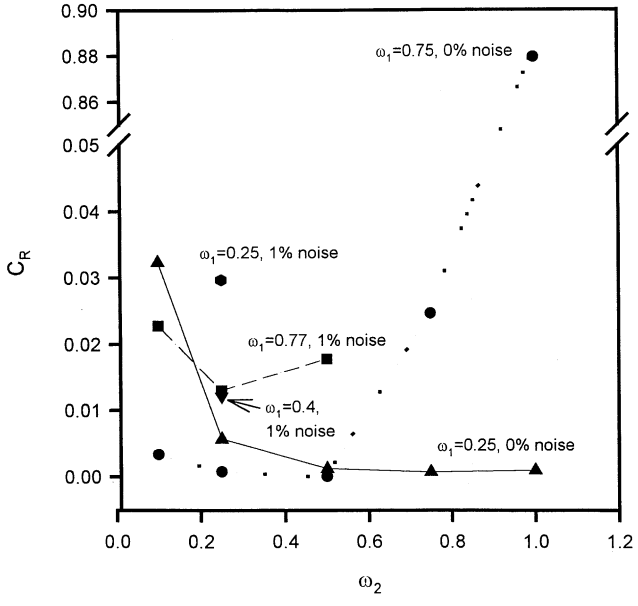

Fig. 12. Values of C_R with noise, for various values of ω_1 and ω_2 around their optimum values for 95 °C simulations.

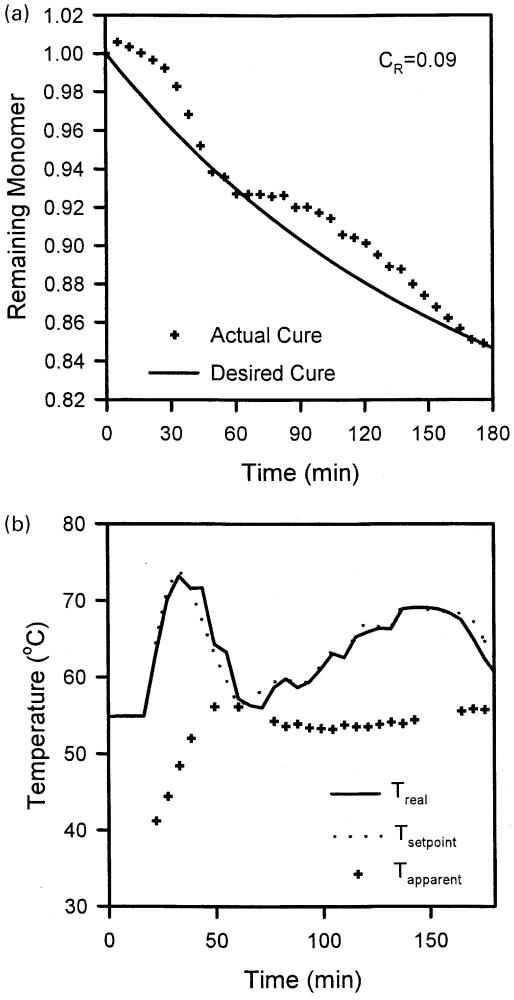

Fig. 13. Experimental data with $\omega_1 = 0.6$ and $\omega_2 = 0.4$, for a programmed temperature of 55 °C. (a) Remaining monomer. (b) Temperature profiles produced by the controller.

compared to the same controller parameters without noise. Note that 1% noise and $\omega_1 = 0.77$ and $\omega_2 = 0.25$ is still the minimum of three different values of ω_2. From this figure and other simulations, it was found that the most effective controller parameters are independent of noise level.

3.6. Experimental results

Experiments were conducted with the HATR cell described earlier with different values of ω_1 and ω_2, at both 55 and 95 °C. All experiments were run with a 1% deadband. Quality of control is again represented by the dimensionless number C_R. Fig. 13 shows cure and temperature data with $\omega_1 = 0.6$ and $\omega_2 = 0.4$, for programmed temperature of 55 °C. The control quality is given by a value of C_R of about 0.09. However, this value is substantially larger than the value of 0.045 predicted by the simulation. This difference may be due to using a deadband slightly smaller than the measurement noise, or from the larger control interval used in the experiments relative to

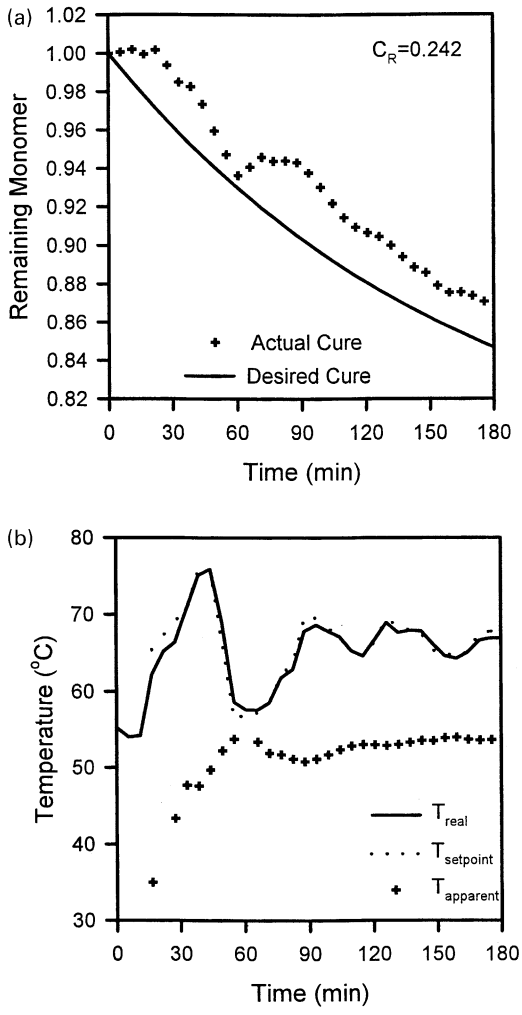

Fig. 14. In an experiment with $\omega_1 = 0.6$ and $\omega_2 = 0.8$, for a programmed temperature of 55 °C, the temperature set-point displays large, stable oscillations, and the value of C_R is substantially larger than shown in Fig. 13. (a) Remaining monomer. (b) Temperature profile produced by the controller.

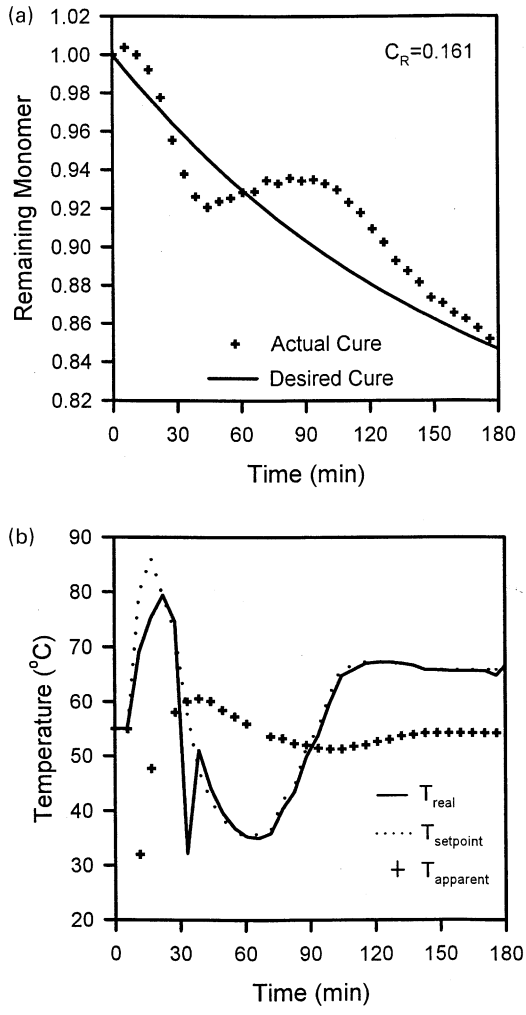

Fig. 15. For values of $\omega_1 = 1.0$ and $\omega_2 = 0.4$, with programmed temperature of 55 °C, there is a large jump in temperature set-point that the heater cannot accommodate. (a) Remaining monomer. (b) Temperature profile produced by the controller.

the simulations. Control was executed every 5 min in the experiment and every 3 min in the simulations. To test this hypothesis, an additional simulation was run with 0% noise at 55 °C, and with a control interval of 5 min. The C_R was degraded by a factor of 2 for the 5 min control interval compared to the 3 min interval, and the C_R value from the simulation run with a 5 min control interval was approximately 0.09, in good comparison with the experiment.

For the more extreme setting of ω_1 and ω_2, the control quality degrades. For the experiment with $\omega_2 = 0.8$ in Fig. 14, the temperature set-point displays large, stable oscillations, and the value of C_R is substantially larger than shown in Fig. 13. This is aggravated by the fact that the mold does not reach the set-point temperature during the specified time interval, calling for an even larger correction the next measurement. An improvement to the control algorithm can take into account limited heating and cooling rates. For the condition of $\omega_1 = 1.0$, as shown in Fig. 15, there is a large jump in temperature set-point that the heater cannot accommodate. Large temperature increases can cause large temperature gradients in the mold from runaway reactions. The optimum temperatures profile should consist of relatively small and gradual temperature changes. As expected, the C_R is poorer than for the more moderate controller parameters.

Control experiments were performed at 95 °C with a 2 min control interval. The achieved control quality is considerably better at 95 °C than at 55 °C for all choices of ω_1 and ω_2. This can be explained by the difference between the control interval for the simulation and experiments. For 95 °C, the control interval for the experiments was one-third shorter than for the simulations, leading to comparable control quality between the simulations and experiments. For 55 °C, the control interval for the experiments was two times the interval for the simulations, which

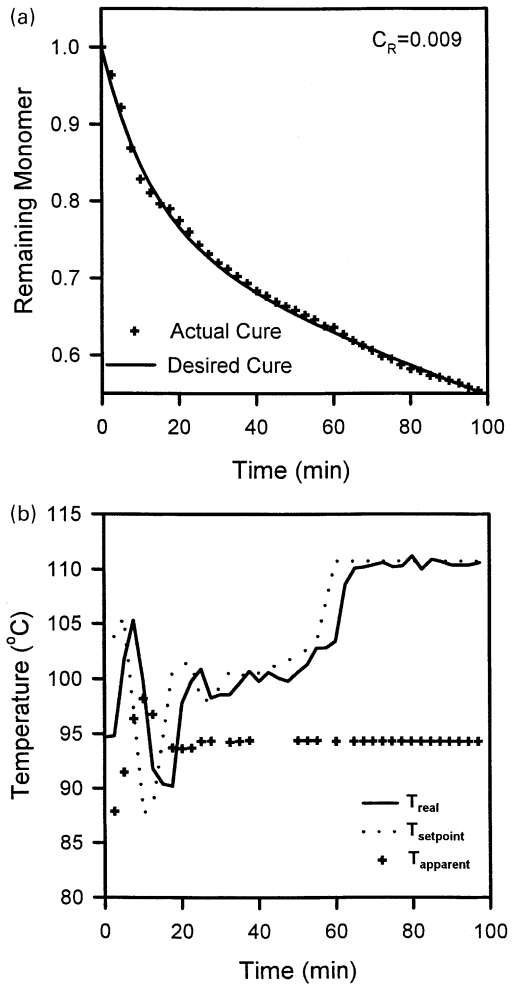

Fig. 16. Experimental data at a programmed temperature of 95 °C using values of $\omega_1 = 1.0$ and $\omega_2 = 0.4$. The mold temperature cannot reach the set-point temperature during the early stages of cure. (a) Remaining monomer. (b) Temperature profile produced by the controller.

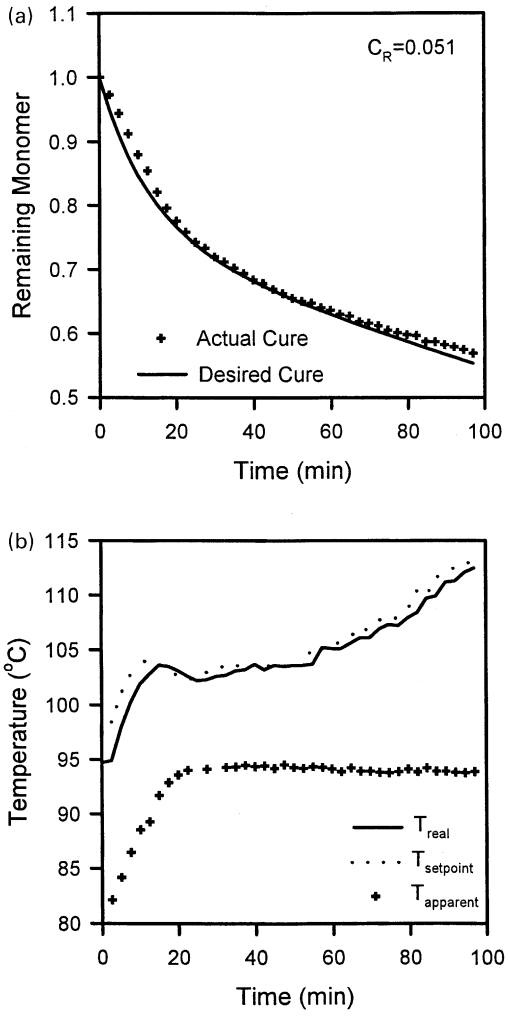

Fig. 17. Experimental data at a programmed temperature of 95 °C using the low values of $\omega_1 = 0.2$ and $\omega_2 = 0.4$. These settings lead to gradual temperature adjustments, but a degraded C_R when compared to Fig. 16. (a) Remaining monomer. (b) Temperature profile produced by the controller.

can account for the degradation of control quality in the experiments compared to the simulations at 55 °C. It should be explained that the same control interval was used for the 55 and 95 °C simulations so the controller robustness between the temperature extremes of the kinetic model could be compared. This control interval is in between the experimental control intervals for the temperatures.

Fig. 16 uses values of $\omega_1 = 1.0$ and $\omega_2 = 0.4$, chosen from Fig. 7. These control parameters are expected to produce good control. In fact, the C_R is excellent. As seen from this figure, however, the mold temperature cannot reach the set-point temperature during the early stages of cure. Lowering ω_1 slightly should produce the same quality of control with more stability in the mold temperature.

Figs. 17 and 18 demonstrate control using nonoptimal settings. Fig. 17 uses the low values of $\omega_1 = 0.2$ and a $\omega_2 = 0.4$. These settings lead to gradual temperature adjustments, but a degraded C_R when compared to Fig. 16. Fig. 18 illustrates results where both ω_1 and ω_2 were set equal to 1.0. The C_R is similar to that achieved in Fig. 16, but the temperature profile is highly undesirable.

4. Conclusions

A model-assisted feedback control algorithm has been developed and implemented with a spectroscopic cure sensor. This controller was found to be robust using the control parameters determined by simulations and experiments for a slowly curing polysiloxane resin system. The controller also performed well under the influence of noise, with up to 10% noise used in the simulations, and approximately 2% noise present in the experiments. Most notably, the values of the most effective tuning parameters appeared uninfluenced by the presence of noise. Control experiments

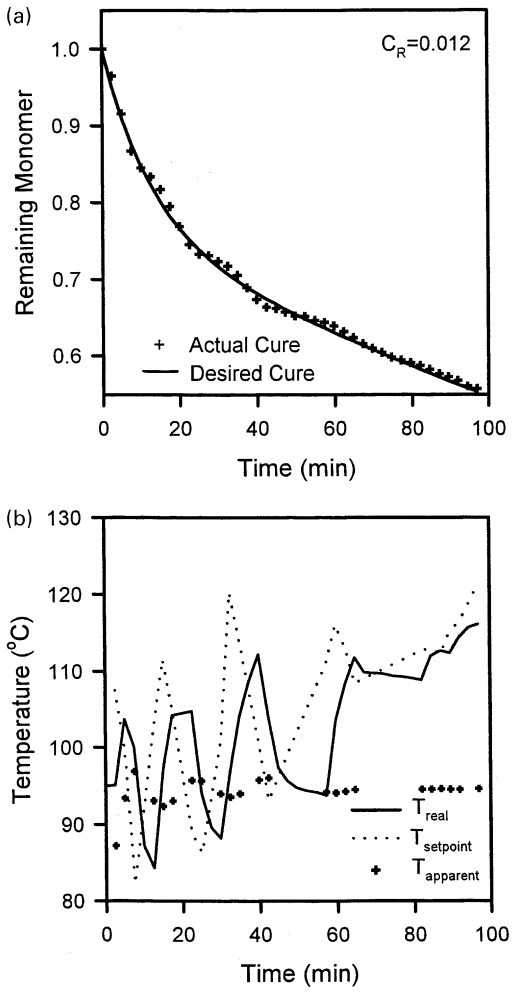

Fig. 18. Experimental results where both ω_1 and ω_2 were set equal to 1.0. The C_R is similar to that achieved in Fig. 16, but the temperature profile is highly undesirable. (a) Remaining monomer. (b) Temperature profile produced by the controller.

verified the trends in controller efficiency established with the simulations. The experiments also demonstrated an acceptable level of control.

5. Disclaimer

Identification of a commercial product is made only to facilitate experimental reproducibility and to adequately describe experimental procedure. In no case does it imply endorsement by NIST or imply that it is necessarily the best product for the experimental procedure.

Acknowledgements

NIST gratefully acknowledges the support by ARPA Technology development Agreement No. MDA972-93-2-0007 that is being administered by the USAF Wright Laboratory Materials Directorate.

References

[1] Sih G. Advanced technology for design and fabrication of composite materials and structures. Dordrecht: Kluwer, 1995.
[2] Kim B, Inoue T. Polymer 1995;36:1985.
[3] Marzcocca A. J Appl Polym Sci 1995;58:1839.
[4] Maistros G, Partridge I. Compos Sci Technol 1995;53:355.
[5] Kranbuehl D, Kingsley P, Hart S. Polym Compos 1994;15:299.
[6] Matsukawa M, Nagai I. J Acoust Soc Am 1996;99:2110.
[7] Mijovic J, Andjelic S. Polymer 1995;36:3783.
[8] Lyon R, Myrick M, Angel S, Vess T. SAMPLE J 1992;28:37.
[9] Druy M, Glatkowski P, Stevenson W. SPIE: Environ Proc Mon Technol 1992:1637.
[10] Liu T, Fernando CF. Compos Part A: Appl Sci Manuf 2001;32:1561.
[11] DeHaseth J, Andrews J, McClusky J, Priester Jr. R, Harthcock M, Davis B. Appl Spectrosc 1993;47:173.
[12] Xu LS, Schlup JR. Appl Spectrosc 1996;50:109.
[13] Xu LS, Shen ZW, Schlup JR. J Adv Mater 1997;28:47.
[14] Zhang BM, Wang DF, Du SY, Song YL. Smart Mater Struct 1999;8:515.
[15] Dunkers JP, Lenhart JL, Kueh SR, van Zanten JH, Advani SG, Parnas RS. Opt Lasers Engng 2001;35:91.
[16] Woerdeman D, Flynn K, Dunkers J, Parnas R. J Rein Plast Compos 1996;15:922.
[17] Dunkers J, Flynn K, Parnas R. Composites Part A 1997;28(A):163.
[18] Marroquin G, Luyben W. Ind Engng Chem Fundam 1972;11:552.
[19] Soroush M, Kravaris C. AIChE J 1992;38:1429.
[20] Soroush M, Valluri S. Proc Am Contr Conf 1994;1:490.
[21] Gattu G, Zafiriou E. Proc Am Contr Conf 1994;1:480.
[22] Thomas M, Kardos J, Joseph B. Proc Am Contr Conf 1994;1:505.
[23] Sourlas D, Naha S, Parnas R, Patterson G. Proc Am Contr Conf 1998:3865.
[24] Voorakaranam S, Joseph B, Kardos JL. J Compos Mater 1999; 33:1173.
[25] Lee P, Sullivan G. Compos Chem Engng 1988;12:573.
[26] Vidyasagar M. Nonlinear systems analysis. New York: Prentice Hall, 1993.
[27] Rudin W. Principles of mathematical analysis. New York: McGraw Hill, 1976.
[28] Dunkers J, Parnas R. 19th Ann Ceram Engng Sci Proc-A 1995:201.
[29] Smith M, Ishida H. Macromolecules 1994;27:2701.
[30] Gardiner C. Handbook of stochastic methods. 2nd ed. New York: Springer, 1985.